# Structure-Based Kinetic Modeling of Excited-State Transfer and Trapping in Histidine-Tagged Photosystem II Core Complexes from Synechocystis †

**ARTICLE** *in* BIOCHEMISTRY · NOVEMBER 2002

Impact Factor: 3.02 · DOI: 10.1021/bi0262597 · Source: PubMed



**4 AUTHORS**, INCLUDING:

Serguei Vassiliev
Brock University
**41** PUBLICATIONS **1,083** CITATIONS
SEE PROFILE

Cheng-I Lee
National Chung Cheng University
**18** PUBLICATIONS **235** CITATIONS
SEE PROFILE

Doug Bruce
Brock University
**73** PUBLICATIONS **1,908** CITATIONS
SEE PROFILE

# Structure-Based Kinetic Modeling of Excited-State Transfer and Trapping in Histidine-Tagged Photosystem II Core Complexes from *Synechocystis*†

Sergei Vassiliev,*,‡ Cheng-I Lee,§ Gary W. Brudvig,§ and Doug Bruce‡

*Department of Biology, Brock University, St. Catharines, Ontario L2S 3A1, Canada, and Department of Chemistry, Yale University, P.O. Box 208107, New Haven, Connecticut 06520-8107*

*Received June 7, 2002; Revised Manuscript Received July 31, 2002*

ABSTRACT: Chlorophyll fluorescence decay kinetics in photosynthesis are dependent on processes of excitation energy transfer, charge separation, and electron transfer in photosystem II (PSII). The interpretation of fluorescence decay kinetics and their accurate simulation by an appropriate kinetic model is highly dependent upon assumptions made concerning the homogeneity and activity of PSII preparations. While relatively simple kinetic models assuming sample heterogeneity have been used to model fluorescence decay in oxygen-evolving PSII core complexes, more complex models have been applied to the electron transport impaired but more highly purified D1−D2−cyt $b_{559}$ preparations. To gain more insight into the excited-state dynamics of PSII and to characterize the origins of multicomponent fluorescence decay, we modeled the emission kinetics of purified highly active His-tagged PSII core complexes with structure-based kinetic models. The fluorescence decay kinetics of PSII complexes contained a minimum of three exponential decay components at $F_0$ and four components at $F_m$. These kinetics were not described well with the single radical pair energy level model, and the introduction of either static disorder or a dynamic relaxation of the radical pair energy level was required to simulate the fluorescence decay adequately. An unreasonably low yield of charge stabilization and wide distribution of energy levels was required for the static disorder model, and we found the assumption of dynamic relaxation of the primary radical pair to be more suitable. Comparison modeling of the fluorescence decay kinetics from PSII core complexes and D1−D2−cyt $b_{559}$ reaction centers indicated that the rates of charge separation and relaxation of the radical pair are likely altered in isolated reaction centers.

Photosystem II (PSII)[1] is a multicomponent pigment−protein complex responsible for catalyzing the light-induced oxidation of water critical to oxygenic photosynthesis. PSII is responsible for supplying reductant to the rest of the photosynthetic electron transport chain via the reduction of plastoquinone (PQ) (*1*). The minimal structure required for charge separation and limited electron transport from appropriate artificial electron donors and acceptors consists of the D1 and D2 polypeptides, cytochrome $b_{559}$, and the PsbI protein and contains six chlorophyll (Chl) and two pheophytin (Pheo) molecules (*2*−*4*). The light harvesting capability of PSII is increased by the association of antenna Chl complexes with the reaction center chromophores. The PSII core complex, capable of water oxidation and quinone reduction, contains the D1−D2−cyt $b_{559}$ reaction center, two Chl binding polypeptides (CP43 and CP47), and several low molecular mass subunits associated with the oxygen-evolving complex (*5*). This functionally active core complex of PSII contains approximately 40 Chl *a* molecules per RC (*6*). In higher plants and green algae PSII is associated with a number of different light harvesting polypeptides (LHC II) which bind Chl *a*, Chl *b*, and carotenoids, and each PSII can be associated with 200−300 antenna Chl molecules (*7*). Light energy absorbed by any Chl associated with PSII generates an excited state that is ultimately transferred to the primary electron donor in the RC (P680). Within the lifetime of the excited state, charge separation (formation of the primary radical pair $P680^+$ and $Pheo^-$) and charge stabilization (reduction of the primary quinone electron acceptor, $Q_A$) occur with greater than 90% efficiency (*8*).

It is widely accepted that charge separation in PSII occurs from a dynamic equilibrium between the primary radical pair and chlorophyll excited states (for review see ref *9*). The reversible radical pair (RRP) kinetic model, first introduced by Schatz et al. (*10*), was successfully used to simulate the fluorescence decay kinetics of PSII particles from cyanobacteria (*10*, *11*). These cyanobacterial PSII preparations included CP43 and CP47 but no LHC II components and were determined, in that study, to contain approximately 80 Chl molecules per P680. The RRP model predicts biphasic decay kinetics for PSII as it assumes that the excited state of the antenna Chl is in equilibrium with the radical pair and that subsequent electron transfer from the radical pair to the primary quinone electron acceptor ($Q_A$) is irreversible (the later assumption is valid on the time scale of measurements and modeling relevant to this study).

† This work has been supported by NSERC. Work at Yale University was supported by the National Institutes of Health (GM32715).

* To whom correspondence should be addressed. E-mail: svassili@spartan.ac.brocku.ca. Phone: (905) 688-5550 ext 4163. Fax: (905) 688-1855.

‡ Brock University.

§ Yale University.

[1] Abbreviations: PS, photosystem; RC, reaction center; Chl, chlorophyll; P680, primary electron donor in photosystem II; Pheo, pheophytin; $Q_A$, primary quinone electron acceptor in photosystem II; PQ, plastoquinone; RP, radical pair; LHC II, light-harvesting complex II; CS, charge separation; DAS, decay-associated spectrum.

10.1021/bi0262597 CCC: $22.00 
Published on Web 09/10/2002

Although the observed decay kinetics were not strictly biphasic, the assumption of some degree of sample heterogeneity allowed the RRP model to provide a reasonably good explanation of the experimental fluorescence decay from samples at both the minimal fluorescence level ($F_0$) associated with open reaction centers (oxidized $Q_A$) and the maximal fluorescence level ($F_m$) associated with closed reaction centers (reduced $Q_A$).

D1−D2−cyt $b_{559}$ reaction center complexes have fewer antenna Chl per reaction center and through more extensive purification procedures are likely to be more homogeneous than PSII core particles from cyanobacteria. Interestingly, these reaction center complexes were found to display more complex multiphasic fluorescence decay kinetics than PSII particles from cyanobacteria (*12*−*14*). Chromophore heterogeneity arising from loss of pigments or pigment photodegradation may be responsible; however, similar complex kinetics are observed in bacterial reaction centers (*15*, *16*). The original RRP model cannot simulate these complex kinetics without the assumption of highly heterogeneous samples.

The original RRP model assumes one value for the free energy difference for radical pair formation ($\Delta G_{RP}$). More complex versions have assumed that samples contain a population of centers which have a static distribution of $\Delta G_{RP}$ that have been suggested to give rise to the multiphasic excited-state dynamics observed in both bacterial reaction centers (*15*, *16*) and D1−D2−cyt $b_{559}$ complexes (*17*, *18*). However, extensive kinetic analysis of the fluorescence decays of isolated D1−D2−cyt $b_{559}$ reaction centers (measured with different combinations of excitation and emission wavelength) confirmed that the assumption of a distribution of $\Delta G_{RP}$ was insufficient to describe the whole kinetic fluorescence data surface (*19*). Again, a distinct kinetically heterogeneous population of PSII had to be invoked to simulate the decay data adequately.

An alternative explanation for the observation of multiexponential fluorescence decay kinetics is that radical pair relaxation may be affected by reorganization of the protein matrix induced by the formation of the radical pair. Reorganization of the protein would be expected to be accompanied by a decrease in the energy level of the radical pair. Changes in the energy level of the radical pair, which occur over the lifetime of the excited state, would increase the complexity of fluorescence decay kinetics. A simulation of fluorescence decay that implemented Förster theory for excitation transfer, and homogeneous and inhomogeneous broadening of the pigment spectra, led to the conclusion that a model with several sequential radical pair energy levels is appropriate for the description of multiple-component experimental kinetics (*20*).

Both sample heterogeneity and changes in the energy level of the radical pair have been used to explain multiexponential fluorescence decay kinetics in D1−D2−cyt $b_{559}$ complexes (*17*−*20*). Surprisingly, fluorescence decay kinetics from PSII core particles, including CP43 and CP47, have rarely been simulated with kinetic models more complex than the original RRP model with its assumption of one static value for $\Delta G_{RP}$. Although both D1−D2−cyt $b_{559}$ complexes and CP43/CP47-containing PSII core complexes exhibit multiexponential decay kinetics, the origin of complexity in the former has most often been assumed to arise from multiphasic trapping kinetics and the latter from sample heterogeneity. There is much evidence for PSII heterogeneity in higher plants. The fluorescence decay kinetics of PSII core complexes from higher plants (*21*), PSII-enriched membrane particles from higher plants (*22*), and thylakoid membranes (*23*) are always more complex than the two-exponential decay assumed by the original RRP model (*22*, *23*). Interpretation of the decay kinetics in these systems is also complicated by the heterogeneous organization of the peripheral PSII antenna and contributions from PSI. It is thus extremely difficult to distinguish between sample heterogeneity, PSII heterogeneity, and the potential multiphasic trapping of excitation by a single PSII reaction center. It is clear that multiple factors could easily be contributing to the complex decay kinetics observed in these systems. To simplify analysis, most earlier studies chose to apply the original single energy level RRP model and assume heterogeneous populations of PSII in the sample (*21*−*23*). However, inspection of the data from these studies shows that this assumption only worked if the contribution of extra decay components (3−8% of the total decay in both the open and closed states of reaction centers) was assigned to uncoupled chlorophylls and excluded from the analysis. This approach was reasonable as the heterogeneous nature of the samples at this time did not allow an unambiguous assignment of the minor components.

What are the origins of multiphasic fluorescence decay kinetics in PSII and how do they relate to the excited-state dynamics? In the present work, we address this question by an analysis of fluorescence decay data from His-tagged PSII core preparations using a kinetic model which assumes a radical pair characterized by either a single energy level, a static distribution of energy levels, or a dynamic energy level. We also apply a heterogeneous model that assumes two populations of reaction centers, each characterized by a radical pair with a single energy level and its own characteristic set of rate constants. The current work has two significant advances over previous studies. The first is the use of highly active and stable His-tagged PSII core preparations with only 40 Chls per reaction center isolated from cyanobacterial mutants with histidine-tagged CP47 (*24*). These preparations exhibit both higher purity (SDS gels) and higher oxygen evolution activity than previous preparations (*25*). The second is the use of a microscopic kinetic model for excitation energy transfer based on the coordinates of antenna and reaction center chromophores (*26*) from the X-ray crystal structure of PSII core complexes from cyanobacteria (*27*). This model has previously shown that the overall excitation trapping rate in PSII is limited by the rate of transfer to the trap, which is in turn sensitive to the spatial arrangement of the chromophores in PSII (*26*).

Our results show that the high-purity histidine-tagged PSII core preparations are characterized by multicomponent decay kinetics. Simulations of the decay data with the structure-based kinetic model strongly support a model that assumes dynamic changes in the energy level of the radical pair.

## MATERIALS AND METHODS

*Sample Preparation.* His-tagged PSII core complexes were prepared using dodecyl $\beta$-D-maltoside solubilization and $Ni^{2+}$ metal affinity chromatography (*25*, *28*). This histidine-tagged PSII preparation has greater purity than previous PSII core

preparations as judged from the high oxygen evolution activity of 2400 $\mu$mol of $O_2$·(mg of Chl)$^{-1}$·h$^{-1}$, SDS−PAGE data (*25*), and high variable fluorescence (see Results).

For fluorescence measurements, samples were diluted using a buffer containing 50 mM Mes−NaOH, 20 mM $CaCl_2$, 5 mM $MgCl_2$, 0.3 M sucrose, and 0.03% (w/v) dodecyl $\beta$-D-maltoside at pH 6.0 to a final Chl concentration of 4 $\mu$M.

*Fluorescence Decay Kinetics*. The samples were excited at 407 nm (PicoQuant PDL-800B pulsed diode laser) at a repetition rate of either 2.5 or 5 MHz for states with open or closed reaction centers, respectively. The instrument response function of the system was 59 ps. For measurements with open reaction centers, the samples were circulated through a 1 mm diameter capillary with a flow rate of about 10 mL/s. To ensure that all reaction centers were open, the samples contained 0.2 mM ferricyanide. The optimal concentration of ferricyanide was determined by titration. It was found that 60 $\mu$M was enough to maintain PSII reaction centers at the open state and further addition of ferricyanide up to 2 mM did not change the decay kinetics. To ensure that $Q_A$ was fully reduced in experiments with closed reaction centers, the incident light intensity was increased, and 1 mM hydroxylamine was added to remove donor-side limitations. The fluorescence decay kinetics did not change during the 20 min acquisition time. Decay kinetics were recorded at seven detection wavelengths between 670 and 700 nm. The data obtained in two time windows of 10 and 25 ns were analyzed globally to obtain lifetimes and corresponding decay-associated spectra (DAS).

*Kinetic Analysis*. For modeling the fluorescence decay kinetics of the His-tagged PSII core complexes, we used the structure-based kinetic model described previously (*26*, *29*). Structure factors ($k^2/R^6$) in the Förster formula (*30*) were calculated from the X-ray PSII coordinate file (PDB ID code 1ILX) (*26*). The overlap integrals were evaluated using the analytical expression of Shipman and Housman (*31*). Spectral assignments were made as described in ref *29* with the exception of the RC chromophores, whose assignment was modified according to ref *32*. To simulate the RP formation, we tested different mechanisms for charge separation. The rate constant for charge recombination $k_{pc}^{-}$ was calculated according to the Boltzmann law:

$$k_{pc}^{-} = k_{pc} \exp\left(-\frac{\Delta G}{k_B T}\right) \qquad (1)$$

Here $k_B$ is the Boltzmann constant, $\Delta G$ is the free energy difference between P680* and RP, and $T$ is the absolute temperature. The static energy level disorder was simulated by ensemble averaging excited-state decay calculations over 1000 reaction centers. For each reaction center calculation, the value of the free energy difference of charge separation ($\Delta G$) was selected randomly from a Gaussian distribution with a mean $\Delta G$ and width $\Gamma$. To include in simulation the effect of the inhomogeneous broadening of the primary radical states, the Marcus nonadiabatic electron transfer theory (*33*) was employed:

$$k_{pc} = \frac{2\pi}{\hbar} V^2 \frac{1}{(4\pi\lambda RT)^{1/2}} \exp\left(\frac{-(\Delta G + \lambda)^2}{4\lambda RT}\right) \qquad (2)$$

Here $V$ is the electronic coupling and $\lambda$ is the reorganization energy. For simulation of the dynamic relaxation of the radical pair, we used the following model: we assumed that primary radical pair $RP_1$ is formed from the excited primary donor P680* with a rate constant $k_{RP_1}$. $RP_1$ is located lower than P680* in energy by $\Delta G_1$, and it relaxes to the next lower energy state $RP_2$. Each RP state can go back to the previous state with a rate constant that can be calculated from eq 1 with corresponding values of $\Delta G_i$ and $k_{RP_i}$. The sum of the rate constants for charge stabilization and other possible nonradiative pathways of the decay of the RP is represented in our model by $k_{ST}$. At $F_0$ $k_{ST}$ is dominated by electron transfer from $Pheo^-$ to $Q_A$. At $F_m$ there is no charge stabilization, and in this case $k_{ST}$ is dominated by the other nonradiative pathways of the decay of the RP such as triplet radical pair formation and/or recombination of the radical pair to the ground state. The values of $\Delta G_i$, $k_{RP_i}$, and $k_{ST}$ at $F_0$ were obtained from target fitting of the fluorescence decay kinetics. For simulation of the $F_m$ data $k_{ST}$ was set to a minimum value 0.02 ns$^{-1}$ in accordance with ref *22*. Up to five states of RP with decreasing energy were included in the model in a manner similar to that previously done for D1−D2−cyt $b_{559}$ simulations (*20*). Data fitting was performed on a LINUX PC cluster using the parallel genetic algorithms library PGAPack.

## RESULTS

*Fluorescence Decay Kinetics.* DAS obtained from global analysis of the data are shown in Figure 1. Decay components of the fluorescence kinetics of His-tagged core complexes with open RC, obtained in our study, are very similar to previous data obtained with core complexes from higher plants (Table 1, data from ref *21*). We found a somewhat faster lifetime of the fast decay component, as compared with PSII particles previously isolated from *Synechococcus* (*10*) with 80 Chls/$P_{680}$. The faster lifetime in this case may be explained either by a higher trapping rate or by the smaller antenna size of our samples (40 Chls/$P_{680}$). We found that the decay kinetics of active His-tagged PSII complexes at $F_0$ could not be described with only two components as had originally been suggested (*11*). Residuals resulting from three- and four-exponential fits to the data are shown in Figure 2. We assign the three decay components with lifetimes of 0.06, 0.26, and 0.97 ns to the active PSII reaction center complexes. The very small 5 ns component is assigned to uncoupled Chls. Van Mieghem et al. (*21*) had previously observed that the decay at $F_0$ was more complex than the two-exponential law. Our data confirm complex fluorescence decay kinetics.

The decay kinetics of the His-tagged PSII core complexes at $F_m$ also could not be described by only two components. The fluorescence decay at $F_m$ was dominated by a long 3.3 ns decay component. In earlier studies the major component of PSII fluorescence decay was reported to have a significantly shorter lifetime of only 1.3−1.5 ns (Table 1), while a component with a lifetime of 3−4 ns was observed as a minor contribution and was attributed to uncoupled chlorophylls or (in case of higher plants) to PSII $\beta$-centers (*34*−*36*). At $F_0$ we observed a very small contribution (1.1%) of uncoupled Chl characterized by a 5.0 ns lifetime and would thus expect the same contribution of this component to be present in the $F_m$ state. This decay component was not

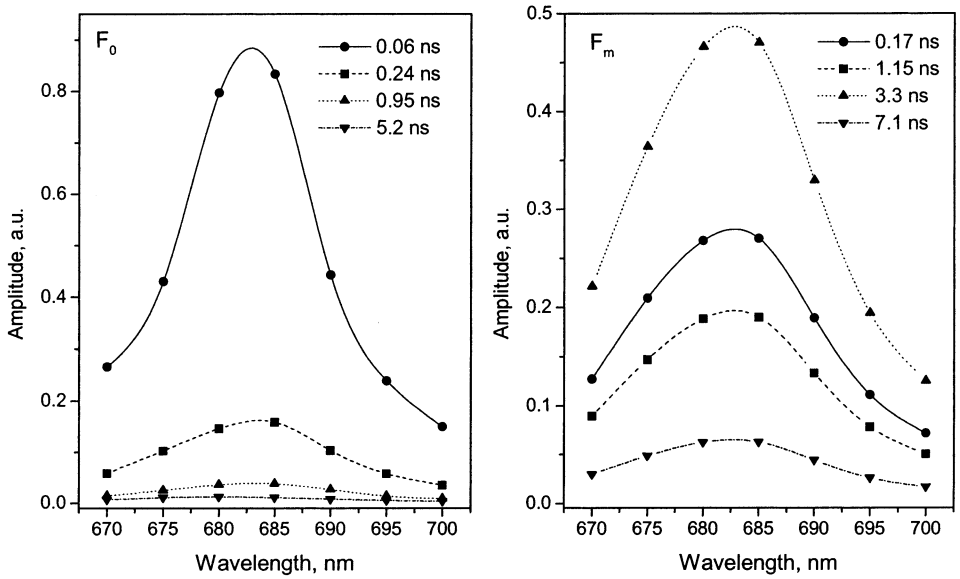


FIGURE 1: Decay-associated spectra of PSII core particles at $F_0$ and $F_m$ as calculated from the amplitudes of the four components used in the global lifetime analysis of the fluorescence decay kinetics.

Table 1: Fluorescence Decay Components Obtained from the Global Lifetime Analysis

| | | $\tau_1$, ns ($A_1$, %) | $\tau_2$, ns ($A_2$, %) | $\tau_3$, ns ($A_3$, %) | $\tau_4$, ns ($A_4$, %) | $F_v/F_0$ |
|---|---|---|---|---|---|---|
| $F_0$ | present study | 0.06 (81) | 0.26 (14.5) | 0.97 (3.4) | 5.0 (1.1) | 22 |
| $F_0$ | data from ref *21* | 0.06 (75) | 0.25 (22) | 0.68 (3) | 3.1 (0.2) | 5.9 |
| $F_0$ | data from ref *10* | 0.08 (72) | 0.52 (20) | 1.8 (8) | | 3.5 |
| $F_m$ | present study | 0.17 (27) | 1.15 (19) | 3.3 (47.7) | 7.9 (6.3) | 22 |
| $F_m$ | data from ref *21* | 0.1 (32) | 0.51 (36) | 1.5 (26) | 4.9 (6) | 5.9 |
| $F_m$ | data from ref *10* | 0.22 (44) | 1.3 (47) | | 4.0 (9) | 3.5 |
| $F_m$ | data from ref *37* | 0.003 (0.19) | 0.021 (57) | 0.1 (14) | >0.1 (10) | |

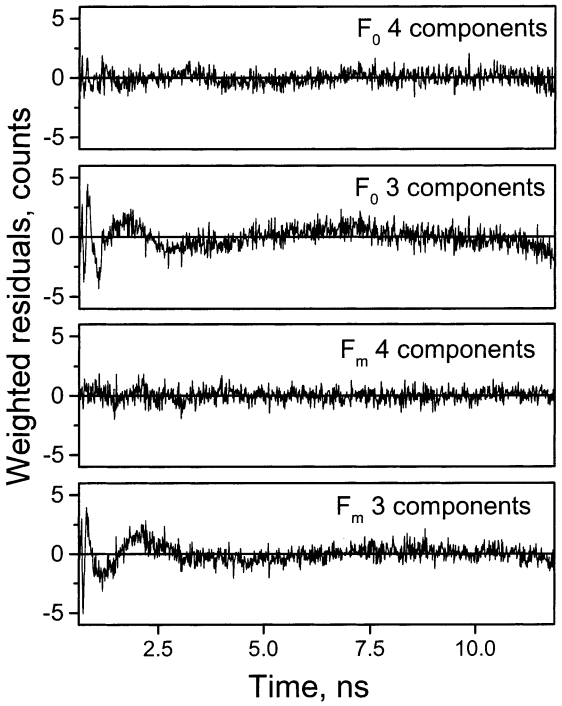


FIGURE 2: Representative weighted residual plots from three- and four-component global lifetime analysis of the fluorescence decay kinetics of PSII core particles at $F_0$ and $F_m$.

resolved at $F_m$, likely due to the dominating presence of the 3.3 and 7.9 ns components, which together made up over 50% of the decay. In the present work, the 3.3 ns component is clearly part of the excited-state decay in active intact PSII reaction centers. The lifetime of this component is very close to the lifetime of Chl *a* in protein in the absence of any photochemical trapping.

Along with the 3.3 ns component, two faster components and one slower were required to describe our data satisfactorily. The fastest component had a longer lifetime (170 ps) than the fast component of the fluorescence decay at $F_0$ (60 ps). If the origin of this component was a small population of open reaction centers still present at $F_m$, it would be expected to have a longer lifetime due to energy transfer between monomers in the PSII dimer. However, it is doubtful that this component arose from residual open centers as its amplitude was not decreased by increases in the incident light intensity, and it is unlikely that such a significant (27%) fraction of open reaction centers would be present in samples with such a large amount of variable fluorescence ($F_v/F_0 =$ 22). The relative contribution of this component was also very reproducible from measurement to measurement. All four components of the fluorescence decay at $F_m$ were thus assigned to PSII.

*Kinetic Analysis.* To simulate radical pair formation in the PSII reaction center, different models for charge separation (Figure 3) were applied. We tested these models for their ability to reproduce the experimental data measured for states with both closed and open reaction centers. Fitting the raw experimental data with the kinetic models would require a computationally expensive convolution of the simulated decay kinetics with the IRF at each iteration step. To reduce the CPU load, we avoided the convolution step by first generating kinetic data from the results of the multiexpo-

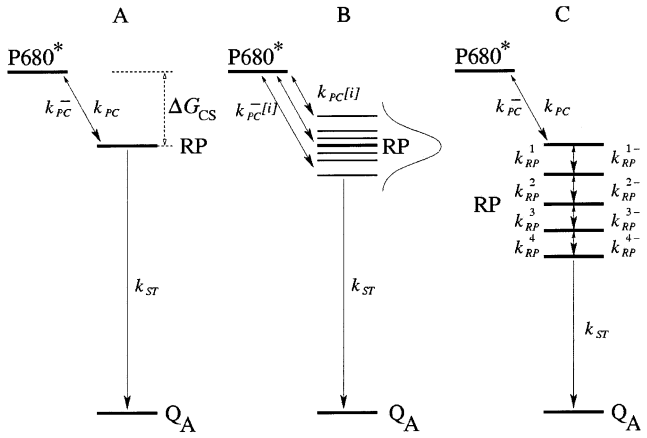


FIGURE 3: Different models of the radical pair formation in the PSII reaction center. (A) One-step formation of the radical pair; the free energy of charge separation $\Delta G_{CS}$ is the same for all RC. (B) One-step radical pair formation with inhomogeneously broadened radical pair energies. (C) Dynamic relaxation of the radical pair energy level.

Table 2: Quality of the Data Fit with Different Charge Separation Models

| kinetic model | $F_0\ \chi^2$ | $F_m\ \chi^2$ |
|---|---|---|
| simple RRP model with fixed $\Delta G_{RP}$ | 3.4 | 10.5 |
| heterogeneous RRP model with fixed $\Delta G_{RP}$ | 2.3[a] | |
| static distribution of the radical pair level | 1.85 | 2.9 |
| sequential radical pair relaxation | | |
| two energy levels | 4.0 | 35 |
| four energy levels | 3.63 | 1.16 |
| five energy levels | 1.19 | 1.07 |

[a] Global.

nential fits to the experimental decay kinetics at 685 nm and adding an appropriate level of noise. These synthetic data were then used for fitting with different kinetic models. The first 5 ps of the decay kinetics, containing contribution from the exciton equilibration within pigment−protein complexes, was not included in analysis of the His-tagged PSII data. The ability of different models to describe the experimental data was judged from the $\chi^2$ values from the fits and is summarized in Table 2.

*Simple Reaction Center Model with a Single Radical Pair and Fixed Radical Pair Energy Level.* Results of our measurements clearly show that the fluorescence decay kinetics are more complex than two exponential for samples with both open and closed reaction centers. We tested the ability of a simple reaction center model with a single radical pair and fixed $\Delta G_{RP}$ to fit the data when employed along with the microscopic excited-state transfer model. In this case, the following fitting parameters were used: the rate constants for charge separation ($k_{PC}$), charge stabilization ($k_{ST}$), and the free energy difference between P680* and the radical pair $\Delta G$.

When this charge separation scheme was applied with the structure-based excited-state transfer model, it was not able to generate a satisfactory description of the experimental decay kinetics (very poor fit quality with this model of both $F_0$ and $F_m$ data; see Table 2).

To account for possible sample heterogeneity in our His-tagged core complexes, we also applied a version of this model which considered two different PSII populations. We performed a global analysis of $F_0$ and $F_m$ data with this

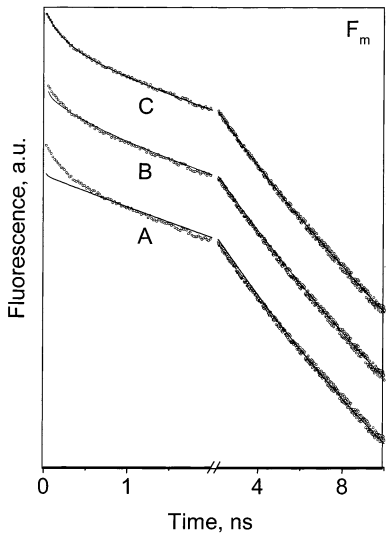


FIGURE 4: Small circles represent fluorescence decay kinetics at $F_m$ generated from the result of the multiexponential fit to the experimental decay kinetics at 685 nm with an appropriate level of noise added. Solid lines are the result of kinetic modeling using models with a fixed $\Delta G_{RP}$ (A), a static distribution of $\Delta G_{RP}$ (B), and a dynamic relaxation of the radical pair energy level (C).

Table 3: Parameters of Radical Pair Formation Obtained from the Model Using a Distribution of Radical Pair Energy Levels

| | $\chi^2$ | $V$ (cm$^{-1}$) | $\lambda$ (cm$^{-1}$) | $\Delta G$ (cm$^{-1}$) | $\Gamma$ (cm$^{-1}$) | $k_{ST}$ (ns$^{-1}$) |
|---|---|---|---|---|---|---|
| $F_m$ | 2.9 | 25 | 455 | −1900 | 2000 | 0.02 |
| $F_0$ | 1.85 | 100 | 1645 | −400 | 900 | 2.6 |

model, taking advantage of the fact that the same relative contribution from the two different kinds of PSII should be present at both $F_0$ and $F_m$ states. We could not fit the experimental data with this model in a satisfactory way (Table 2, $\chi^2 = 2.3$). Not only was the fit quality poor, but all solutions found by the fitting routine for the $F_m$ decay required the use of a very large $k_{ST}$ (>1.5 ns$^{-1}$) for a significant fraction (>40%) of reaction centers.

*Electron Transfer Model with a Static Distribution of the Radical Pair Energy Level.* In a second step, we adapted the single radical pair model with fixed $\Delta G_{RP}$ to include energetic disorder of the radical pair energy level. Such disorder is a common feature, observed for chromophores embedded in protein matrices. It is expected to arise from the differences in the local protein environment of the chromophores of the primary radical pair.

The fitting parameters used with this model were the electronic coupling $V$, the free energy difference between P680* and RP, $\Delta G$, and the reorganization energy $\lambda$ (see eq 2). The quality of the fit with this model was significantly improved) but still not satisfactory to describe $F_m$ data (Figure 4). The parameters for radical pair formation obtained from the model with a distribution of radical pair energy levels are summarized in Table 3. The quantum yield of $Q_A$ reduction calculated with the best fit parameters of this model was only 30%.

*Electron Transfer Model with a Dynamic Relaxation of the Radical Pair.* Models assuming a dynamic relaxation of the radical pair are capable of describing multiexponential decays. The origin of the complex decay kinetics can be understood for this case as follows: the fast decay component represents excitation loss due to initial charge separation,

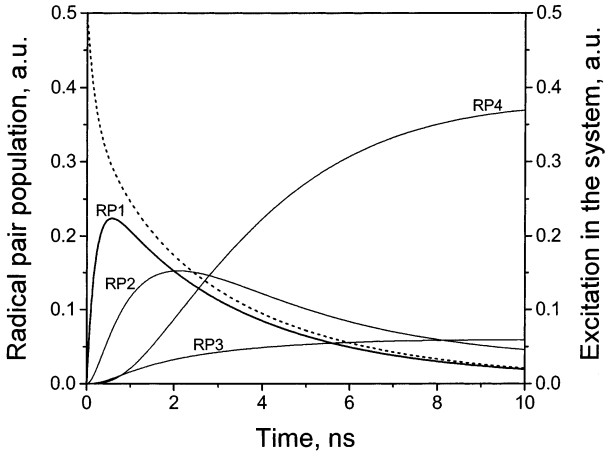


FIGURE 5: Representative time dependencies of the population of the four radical pair states obtained from the best fit of the $F_m$ decay kinetics using the sequential RP relaxation model with four RP energy levels (solid lines) and the excited-state decay kinetics of His-tagged PSII core complexes (dashed line).

when the primary (unrelaxed) RP is not yet populated. When a sufficient amount of the primary RP is formed, the excited state will become repopulated from recombination of this unrelaxed RP. If only one radical pair level exists, the radical pair will decay exponentially, giving rise to the slower excited-state decay component. However, when several sequentially relaxing radical pair states are present, each of the subsequent RP states will repopulate the previous state via back-reactions leading to a progressive deviation of the decay of the first unrelaxed RP and the recombinational excited-state decay component from a single-exponential law. The excited-state decay will thus ultimately depend on the dynamic equilibrium between all possible radical pair states. The representative time dependencies of population of the four radical pair states and the excited state are shown for $F_m$ in Figure 5.

A model with only two sequential radical pairs was not sufficient to describe the data. The best fits for this case were characterized by $\chi^2$ values of 4.0 and 35.0 for the $F_0$ and $F_m$ states, respectively (Table 2). Four sequential radical pairs were also insufficient to fit the data (Table 2). With five sequential radical pair energy levels, the quality of the fit was greatly improved compared to the model with the static distribution or models with fewer sequential radical pairs. We also applied this sequential relaxation model to the analysis of fluorescence decay kinetics of D1−D2−cyt $b_{559}$ complexes taken from the literature (*37*). Parameters arising from all decay simulations generated with this model are compiled in Table 4.

The quantum yield of $Q_A$ reduction calculated with the best parameter values for this model was 98%. Thus, as opposed to the static disorder model, the dynamic relaxation model was capable of describing multiexponential decays and predicting a high yield of $Q_A$ reduction.

## DISCUSSION

We found that the fluorescence decay kinetics of His-tagged PSII core complexes with both open and closed reaction centers are multiphasic. We assigned the multiphasic decays to active PSII reaction centers and fit them with different kinetic models. Multiphasic fluorescence decays from PSII core complexes have been observed in previous studies but were assumed to arise from sample heterogeneity. Even though it had been suggested that heterogeneity of the sample with respect to the primary photochemical reactions was responsible for the complex decay kinetics (*21*), no attempts to analyze the nature of the multiexponential decay of PSII core complexes with kinetic models have been made. Our present study has done this with data from highly active His-tagged PSII core complexes and X-ray structure based kinetic models.

An interesting finding of our present study was that PSII fluorescence decay at $F_m$ was significantly slower than previously observed in other PSII preparations. As $Q_A$ is reduced at $F_m$, no charge stabilization is possible, and the slow component of fluorescence decay in closed centers would be expected to approach the intrinsic fluorescence lifetime of Chl in protein (about 3 ns). This fits quite well with the 3.3 ns component dominating our $F_m$ data. However, the $F_m$ decay in previous work has been characterized by a 1.0−1.5 ns decay component. These shorter lifetimes were explained in previous kinetic models by assuming an increase in the rate of radiationless decay of the radical pair (by a factor of 2 or 3) at $F_m$ as compared to $F_0$ (*34*). However, there is no clear physical reason to justify this change, and our current data and model do not require this assumption.

We have applied a structure-based kinetic model for excitation energy transfer coupled to a number of different schemes of charge separation for the analysis of the fluorescence decay kinetics at both $F_0$ and $F_m$ levels. We found that a single radical pair model with fixed $\Delta G_{RP}$ failed to reproduce the decay kinetics of His-tagged PSII core complexes with either open or closed reaction centers. This is in accord with previous observations that the original RRP model with fixed $\Delta G_{RP}$ fails to reproduce the antenna size dependence of the trapping of excitation by closed PSII reaction centers (*37*).

We cannot exclude that some sort of heterogeneity exists in His-tagged PSII core complexes. We believe, however, that it is not likely that sample heterogeneity is responsible for multiexponential decay kinetics. Our first argument is that, despite the higher purity and activity of His-tagged core complexes compared to previously studied PSII preparations (*11*, *21*), there is no indication that the decay kinetics of His-tagged PSII core complexes are less complex. We also attempted to fit our data with two different types of heterogeneous kinetic models: one type assumed a Gaussian population of RP energy levels, and the other assumed two PSII populations, each characterized by its own set of rate constants. Neither of these models was able to describe the experimental decay kinetics in a satisfactory manner.

Our simulations show that models with a static distribution or a dynamic relaxation of the radical pair are both able to describe the measured fluorescence decay kinetics at $F_0$. The static energy disorder model, however, is not acceptable for the description of charge separation in PSII for several reasons:

(i) The distribution of the RP energy level has to be unrealistically broad with a half-width of about 2000 cm $^{-1}$ at $F_m$ or 900 cm $^{-1}$ at $F_0$ to reproduce the experimental data. The width of the distribution is significantly broader than the experimentally determined width of the radical pair $P680^+Pheo$ transient absorption spectrum (210 $cm^{-1}$) (*38*)

Table 4: Parameters of Radical Pair Formation Obtained from the Model Using Sequential Radical Pair Relaxation

| | PSII core, $F_0$ | | | PSII core, $F_m$ | | | D1−D2 RC[a] | | |
|---|---|---|---|---|---|---|---|---|---|
| | $k_{RP_i}$ ($ns^{-1}$) | $\Delta G_i$ ($cm^{-1}$) | $\Delta G_i$ (meV) | $k_{RP_i}$ ($ns^{-1}$) | $\Delta G_i$ ($cm^{-1}$) | $\Delta G_i$ (meV) | $k_{RP_i}$ ($ns^{-1}$) | $\Delta G_i$ ($cm^{-1}$) | $\Delta G_i$ (meV) |
| $P680^*-RP_1$ | 7400 | −464 | −58 | 11.7 | −242 | −30 | 80 | −540 | −67 |
| $RP_1-RP_2$ | 1200 | −91 | −11 | 0.97 | −210 | −26 | 0.6 | −241 | −30 |
| $RP_2-RP_3$ | 1090 | −26 | −3.2 | 0.77 | −224 | −28 | 1.5 | −97 | −12 |
| $RP_3-RP_4$ | 252 | −179 | −22 | 0.63 | −272 | −34 | 2.8 | −374 | −46 |
| $RP_4-RP_5$ | 4.6 | −585 | −73 | 8.2 | −312 | −39 | 3.1 | −210 | −26 |
| total | | | −167 | | | −157 | | | −181 |

[a] Data from ref *37*.

or the inhomogeneous broadening of P680 absorption bands (100 $cm^{-1}$) (*20*).

(ii) The most important reason for rejection of this model is that it is unable to predict a high quantum yield for $Q_A$ reduction. Even for reaction centers with radical pair energy levels at the peak of the distribution, the yield of $Q_A$ reduction was only 65%. After averaging over the whole distribution, the yield of $Q_A$ reduction was only approximately 30%. These numbers are in contradiction with the experimentally observable quantum yield of more than 95% (*8*).

A similar reaction center model with two distributed radical pairs was previously applied to describe antenna-size dependence of the fluorescence yield in PSII particles of varying antenna size (*37*). The model was only applied to analysis of data acquired with closed reaction centers ($F_m$), and broad distributions of the radical pair states were required to describe the data. Results of our simulations show that if such broad distributions of the radical pair energy levels existed in open reaction centers, the PSII quantum yield would be very low. Despite the fact that the static energy disorder model with two distributed RP states describes energy trapping in a variety of PSII preparations correctly, its application is obviously limited to closed reaction centers.

Along with energetic disorder, dynamic relaxation processes are involved in electron transfer (*19, 20*). An unrelaxed radical pair is thought to be formed as a product of charge separation. Then relaxation of this radical pair takes place via a series of small downhill steps involving charge-induced movements of chromophores, side chains of amino acids, and/or other changes in the protein conformation. Such relaxation is important for quickly lowering the radical pair energy level, which makes the reverse reaction much slower than the forward and thus contributes to the high overall efficiency of photochemistry.

Using this model, we were able to achieve the best description of the decay kinetics at both $F_0$ and $F_m$ levels. A total value for $\Delta G$ of about −157 meV at $F_m$ and about −167 meV at $F_0$ was required to fit the data. Although higher than the experimentally estimated value of about −100 meV (*39*−*41*), it is much closer than the prediction of static disorder models, as shown in this work and ref *15*. In contrast to static disorder models, the dynamic relaxation model was able to predict a high yield of $Q_A$ reduction in addition to describing multiexponential fluorescence decay kinetics.

Application of the sequential relaxation model to the analysis of the fluorescence decay kinetics of D1−D2−cyt $b_{559}$ complexes enabled us to address the question of whether rates of photochemical processes are modified in the D1−D2−cyt $b_{559}$ complexes compared to intact His-tagged PSII core complexes. D1−D2−cyt $b_{559}$ complexes perform charge separation, but without $Q_A$ present there is no charge stabilization reaction. In the absence of added electron acceptors the charge-separated state will thus either recombine or relax nonradiatively, similar to PSII core complexes at $F_m$. If primary charge separation is not affected by the isolation procedure, the same model with some insignificant changes of parameters (presumably only changes of $k_{RP_1}$) would be sufficient to describe the kinetics of both types of PSII preparations. It is expected that the rate of charge separation would be higher in D1−D2−cyt $b_{559}$ complexes due to the absence of the electrostatic repulsion between $Q_A^-$ and $Pheo^-$, and the radical pair relaxation rate could be retarded as well. Results of the modeling are shown in Table 4. Our kinetic simulations revealed that $k_{PC}$ is a factor of 8 higher in D1−D2−cyt $b_{559}$ than in His-tagged PSII core complexes at $F_m$. This value of the charge separation rate, however, is still about 2 orders of magnitude smaller than the rate of charge separation determined for the His-tagged PSII core complexes at the $F_0$ state, indicating that this process in isolated D1−D2−cyt $b_{559}$ complexes is significantly retarded. Recent assignment of the $Q_Y$ absorbance bands of intact photosystem II chromophores revealed significant shifts of energy levels of the RC chromophores in D1−D2−cyt $b_{559}$ complexes compared to intact PSII core complexes (*32*). The present analysis shows that not only are energy levels affected by the isolation procedure but the rates of charge separation and relaxation of the radical pair as well.

Most recent work on the D1−D2−cyt $b_{559}$ complexes has measured multiphasic decays and assumed homogeneous samples with multiphasic trapping kinetics as the source. In this study we have shown that a similar approach could be applied to the larger PSII core preparations, especially ones with such high purity and high activity. The one assumption, that of a dynamic energy level of the radical pair, was enough to fit both $F_0$ and $F_m$ data and explain the different relative contributions of multiphasic decay at $F_0$ (relatively small) and $F_m$ (relatively large) without invoking any heterogeneity.

The results of our study show that both static disorder and dynamic relaxation of the RP may be present, but dynamic relaxation prevails in open reaction centers when photochemistry is active and fast stabilization of the radical pair is a requirement for high quantum yield.

## REFERENCES

1. Barry, B. A., Boerner, R. J., and de Paula, L. C. (1994) in *The Molecular Biology of Cyanobacteria* (Bryant, D. A., Ed.) pp 217−257, Kluwer Academic Publishers, Dordrecht.
2. Kobayashi, M., Maeda, H., Watanabe, T., Nakane, H., and Satoh, K. (1990) *FEBS Lett. 260*, 138−140.

3. Gounaris, K., Chapman, D. J., Booth, P., Crystall, B., Giorgi, L., Klug, D., Porter, G., and Barber, J. (1990) *FEBS Lett. 265*, 88−92.
4. van Leeuwen, P. J., Nieveen, M. C., van de Meent, E. J., Dekker, J. P., and Van Gorkom, H. J. (1991) *Photosynth. Res. 28*, 149−153.
5. Hankamer, B., Barber, J., and Boekema, E. J. (1997) *Annu. Rev. Plant Physiol. Plant Mol. Biol. 48*, 641−671.
6. Ohno, T., Satoh, K., and Katoh, S. (1986) *Biochim. Biophys. Acta 852*, 1−8.
7. Bassi, R., Pineau, B., Dainese, P., and Marquardt, J. (1993) *Eur. J. Biochem. 212*, 297−303.
8. Hou, J.-M., Boichenko, V. A., Diner, B. A., and Mauzerall, D. (2001) *Biochemistry 40*, 7117−7125.
9. Dekker, J. P., and van Grondelle, R. (2000) *Photosynth. Res. 63*, 195−208.
10. Schatz, G. H., Brock, H., and Holzwarth, A. R. (1987) *Proc. Natl. Acad. Sci. U.S.A. 84*, 8414−8418.
11. Schatz, G. H., Brock, H., and Holzwarth, A. R. (1988) *Biophys. J. 54*, 397−405.
12. Greenfield, S. R., Seibert, M., Govindjee, and Wasielewski, M. R. (1997) *J. Phys. Chem. B 101*, 2251−2255.
13. Donovan, B., Walker, L. A., Kaplan, D., Bouvier, M., Yocum, C. F., and Sension, R. J. (1997) *J. Phys. Chem. 101*, 5232−5238.
14. Klug, D. R., Durrant, J. R., and Barber, J. (1998) *Philos. Trans. R. Soc. London, Ser. A 356*, 449−464.
15. Ogrodnik, A., Keupp, W., Volk, M., Aumeier, G., and Michel-Beyerle, M. E. (1994) *J. Phys. Chem. 98*, 3432−3439.
16. Wang, Z., Pearlstein, R. M., Jia, Y., Fleming, G. R., and Norris, J. R. (1993) *Chem. Phys. 176*, 421−425.
17. Booth, P., Crystall, B., Ahmad, I., Barber, J., Porter, G., and Klug, D. (1991) *Biochemistry 30*, 7573−7586.
18. Groot, M. L., Peterman, E. J. G., van Kan, P. J. M., van Stokkum, I. H. M., Dekker, J. P., and van Grondelle, R. (1994) *Biophys. J. 67*, 318−330.
19. Gatzen, G., Müller, M. G., Griebenow, K., and Holzwarth, A. R. (1996) *J. Phys. Chem. 100*, 7269−7228.
20. Konermann, L., Gatzen, G., and Holzwarth, A. R. (1997) *J. Phys. Chem. 101*, 2933−2944.
21. van Mieghem, F. J. E., Searle, G. F. W., Rutherford, A. W., and Schaafsma, T. J. (1992) *Biochim. Biophys. Acta 1100*, 198−206.
22. Vass, I., Gatzen, G., and Holzwarth, A. R. (1993) *Biochim. Biophys. Acta 1183*, 388−396.
23. Dau, H., and Sauer, K. (1996) *Biochim. Biophys. Acta 1273*, 175−190.
24. Bricker, T. M., Morvant, J., Mastri, N., Sutton, H. M., and Frankel, L. K. (1998) *Biochim. Biophys. Acta 1409*, 50−57.
25. Lakshmi, K. V., Reifler, M. J., Crishholm, D. A., Wang, J. Y., Diner, B. A., and Brudvig, G. W. (2002) *Photosynth. Res. 72*, 175−189.
26. Vasil'ev, S., Orth, P., Zouni, A., Owens, T. G., and Bruce, D. (2001) *Proc. Natl. Acad. Sci. U.S.A. 98*, 8602−8607.
27. Zouni, A., Witt, H.-T., Kern, J., Fromme, P., Krauss, N., Saenger, W., and Orth, P. (2001) *Nature 409*, 739−743.
28. Reifler, M. J., Chisholm, D. A., Wang, J. Y., Diner, B. A., and Brudvig, G. W. (1998) in *Photosynthesis: Mechanisms and Effects* (Garab, G., Ed.) pp 1189−1192, Kluwer Academic Publishers, Dordrecht.
29. Vasil'ev, S., and Bruce, D. (2000) *Biochemistry 39*, 14211−14218.
30. Förster, T. (1965) in *Modern Quantum Chemistry* (Sinanoglu, O., Ed.) Vol. III, pp 93−137, Academic Press, New York.
31. Shipman, L. L., and Housman, D. L. (1979) *Photochem. Photobiol. 29*, 1163−1167.
32. Stewart, D. H., Nixon, P. J., Diner, B. A., and Brudvig, G. W. (2000) *Biochemistry 39*, 14583−14594.
33. Marcus, R. A., and Sutin, N. (1985) *Biochim. Biophys. Acta 811*, 265−322.
34. Roelofs, T. A., Lee, C.-H., and Holzwarth, A. R. (1992) *Biophys. J. 61*, 1147−1163.
35. Wagner, B., Goss, R., Richter, M., Wild, A., and Holzwarth, A. R. (1996) *J. Photochem. Photobiol., B 36*, 339−350.
36. Richter, M., Goss, R., Wagner, B., and Holzwarth, A. R. (1999) *Biochemistry 38*, 12718−12726.
37. Barter, L. M. C., Bianchietti, M., Jeans, C., Schilstra, M. J., Hankamer, B., Diner, B. A., Barber, J., Durrant, J. R., and Klug, D. (2001) *Biochemistry 40*, 4026−4034.
38. Groot, M. L., van Mourik, F., Eijckelhoff, C., van Stokkum, I. H. M., Dekker, J. P., and van Grondelle, R. (1997) *Proc. Natl. Acad. Sci. U.S.A. 94*, 4389−4394.
39. Van Dorssen, R. J., Breton, J., Plijter, J. J., Satoh, K., Van Gorkom, H. J., and Amesz, J. (1987) *Biochim. Biophys. Acta 893*, 267−274.
40. Volk, M., Gilbert, M., Rousseau, G., Richter, M., Ogrodnik, A., and Michel-Beyerle, M. E. (1993) *FEBS Lett. 336*, 357−362.
41. Booth, P., Crystall, B., Giorgi, L., Barber, J., Klug, D., and Porter, G. (1990) *Biochim. Biophys. Acta 1016*, 141−152.

BI0262597